

# Microwave sky and the local Rees–Sciama effect

Aleksandar Rakić<sup>1\*</sup>, Syksy Räsänen<sup>2†</sup> and Dominik J. Schwarz<sup>1‡</sup>

<sup>1</sup>*Fakultät für Physik, Universität Bielefeld, Postfach 100131, D-33501 Bielefeld, Germany*

<sup>2</sup>*CERN, Physics Theory Department, CH-1211 Geneva 23, Switzerland*

Accepted 2006 March 9. Received 2006 March 1; in original form 2006 January 25

## ABSTRACT

The microwave sky shows unexpected features at the largest angular scales, among them the alignments of the dipole, quadrupole and octopole. Motivated by recent X-ray cluster studies, we investigate the possibility that local structures at the  $100 h^{-1}\text{Mpc}$  scale could be responsible for such correlations. These structures give rise to a local Rees–Sciama contribution to the microwave sky that may amount to  $\Delta T/T \sim 10^{-5}$  at the largest angular scales. We model local structures by a spherical overdensity (Lemaître–Tolman–Bondi model) and assume that the Local Group is falling toward the centre. We superimpose the local Rees–Sciama effect on a statistically isotropic, gaussian sky. As expected, we find alignments among low multipoles, but a closer look reveals that they do not agree with the type of correlations revealed by the data.

**Key words:** cosmic microwave background, large-scale structure of Universe

The microwave sky has presented some surprises at the largest angular scales. The Wilkinson Microwave Anisotropy Probe (WMAP) confirmed the vanishing of the angular two-point correlation function above  $60^\circ$  (Bennett et al. 2003a), a result first obtained by the Cosmic Background Explorer’s Differential Microwave Radiometer (COBE-DMR) experiment (Hinshaw et al. 1996). In terms of the angular power spectrum this implies that the quadrupole and octopole are below the theoretical expectation.

The analysis of full-sky maps that have been cleaned from foreground (Bennett et al. 2003b), (Tegmark, de Oliveira-Costa & Hamilton 2003), (Eriksen et al. 2004b) has revealed further surprises. It was pointed out by de Oliveira-Costa et al. (2004) that the octopole seems to be planar (all minima and maxima are close to a great circle on the sky) and the planes of the octopole and the quadrupole are closely aligned. Eriksen et al. (2004a) showed that the northern galactic hemisphere lacks power compared with the southern hemisphere. By means of multipole vectors (Copi, Huterer & Starkman 2004), Schwarz et al. (2004) showed that the quadrupole and octopole are correlated with each other and with the orientation and motion of the Solar system. The four cross products of the quadrupole and octopole vectors are unexpectedly close to the ecliptic [ $> 98\%$  confidence level (C.L.)] as well as to the equinox (EQX) and microwave dipole (both  $> 99.7\%$  C.L.) (Copi et al. 2005). Based on

the additional alignment of a nodal line with the ecliptic and an ecliptic north–south asymmetry of the quadrupole plus octopole map, Copi et al. (2005) argued that the correlation with the ecliptic is unlikely at the  $> 99.9\%$  C.L. In contrast to an unknown Solar system effect, it also seems possible that the large-scale anomalies are due to a physical correlation with the dipole, in which case the correlation with the ecliptic and the EQX would be due to the accidental closeness of the dipole and the EQX.

In this letter we explore the possibility that the effect of local non-linear structures on the cosmic microwave background (CMB), the local Rees–Sciama (RS) effect (Rees & Sciama 1968), could induce a correlation between the dipole and higher multipoles. In the non-linear regime of large-scale structure formation the gravitational potential changes with time, and photons climb out of a potential well slightly different from the one they fell into. As the CMB dipole is considered to be due to our motion with respect to the CMB rest frame, and this motion is due to the gravitational pull of local structures, these structures are a natural candidate for contributions to the higher multipoles correlated with the dipole. Earlier work on the effects of large nearby structures on the CMB includes the moving cluster of galaxies effect (Vale 2005; Cooray & Seto 2005), which is different from the effect we are considering here. Second order corrections to the integrated Sachs–Wolfe effect, which catch some aspects of the local RS effect have been considered by Tomita (2005a, 2005b).

The RS effect of distant clusters was estimated to be at most  $10^{-6}$  in a matter-dominated Universe in Seljak (1996), one order of magnitude below the intrinsic CMB anisotropy. The effect of local large structures has been

\* E-mail: rakic at physik dot uni-bielefeld dot de

† E-mail: syksy dot rasanen at iki dot fi

‡ E-mail: dschwarz at physik dot uni-bielefeld dot de

estimated to be at most  $10^{-6}$  using the Swiss Cheese model (Martínez-González & Sanz 1990) and, more reliably, the Lemaitre–Tolman–Bondi (LTB) model, which is the general spherically symmetric dust solution of the Einstein equation (Panek 1992; Sáez, Arnau & Fullana 1993; Fullana, Sáez & Arnau 1994). For an overview, see Krasiński (1997).

At the time these studies were made, it was generally thought that the dipole is mostly due to the infall of the Local Group (LG) of galaxies towards the Great Attractor (GA) (Lynden-Bell et al. 1988; Dressler 1988), a density concentration located 40–60  $h^{-1}$ Mpc from us, with a subdominant component due to the nearby Virgo cluster, about 10  $h^{-1}$ Mpc away. Recent observations of X-ray clusters suggest instead that there is a major contribution to the dipole from the Shapley Supercluster (SSC) and other density concentrations at a distance of around 130–180  $h^{-1}$  Mpc (Kocevski, Mullis & Ebeling 2004; Hudson et al. 2004; Lucey, Radburn-Smith & Hudson 2004; Kocevski & Ebeling 2005). The SSC alone has a density contrast of  $\approx 5$  over a 30  $h^{-1}$ Mpc region (Proust et al. 2005), which is 2–3 times the size of the core (of similar density) in the GA models.

An SSC-like object could induce anisotropies at the  $10^{-5}$  level, consistent with an early estimate in Martínez-González & Sanz (1990). This can be understood by the approximate scaling (Panek 1992)

$$\Delta T/T \sim \delta^{3/2}(d/t)^3, \quad (1)$$

where  $\delta$  is the density contrast of the structure,  $d$  is its size and  $t$  is the time at which the CMB photons crossed it. For a large angular scale of the source (local and nearby structures), this induces contributions to low- $\ell$  multipoles, especially the dipole, quadrupole and octopole. This could include a non-Doppler contribution to the dipole. This would imply a change of a few percent in the inferred dipole velocity, which might also explain some of the CMB anomalies (Freeman et al. 2005). The SSC is a non-linear structure, and the amplitude of the induced anisotropies cannot be reliably calculated in linear perturbation theory. According to a comparison of linear and exact calculations for GA-like objects with the LTB model in Fullana et al. (1994), linear theory is reliable at distances comparable to the Hubble scale, but fails for structures within 1000  $h^{-1}$ Mpc or so.

The advantage of the spherical symmetry of the LTB model is that it allows exact calculations for non-linear objects; the drawback is that the observed non-linear objects such as the GA and SSC do not appear to be spherically symmetric. However, one would expect the result to be correct within an order of magnitude, and the core of the SSC does seem to be roughly spherical (Proust et al. 2005). Also, if the preferred direction indicated by the low- $\ell$  anomalies is due to local structures, this implies that there indeed *is* a degree of symmetry in the local mass distribution.

In addition, there is a second motivation for studying a spherically symmetric inhomogeneous model, namely dark energy. If interpreted in the framework of isotropic and homogeneous cosmology, observations of SNIa imply that the expansion of the Universe is accelerating. However, in an inhomogeneous spacetime the observations are not necessarily inconsistent with deceleration. In particular, in the LTB model the parameter  $q_0$  defined with the

**Table 1.** Directions of local motion with respect to the CMB rest frame. Estimated error for the corrected LG direction of Plionis & Kolokotronis (1998)(PK) is  $14^\circ$ , and is 5% for the velocities.

Direction	Galactic coordinates	$V$ [km/s]
WMAP dipole velocity [Bennett et al. (2003a)]	$l = 263^\circ 85 \pm 0^\circ 10$ $b = 48^\circ 25 \pm 0^\circ 04$	(368±2)
LG velocity [Kogut et al. (1993)]	$l = 276^\circ \pm 3^\circ$ $b = 30^\circ \pm 3^\circ$	(627±22)
Virgo infall of LG [PK (1998)]	$l = 283^\circ 92$ $b = 74^\circ 51$	170
Virgo corrected LG vel. [PK (1998)]	$l = 276^\circ$ $b = 16^\circ$	510
Shapley concentration [Einasto et al. (1997)]	$l = 306^\circ 44$ $b = 29^\circ 71$	-

luminosity distance is no longer a direct measure of acceleration (Humphreys, Maartens & Matravers 1997). It has been suggested by several groups that a spherically symmetric inhomogeneity could be used to explain the SNIa data (Célérier 1999; Tomita 2001; Alnes, Amarzguioui & Gron 2005), though it is not clear whether such a model could be consistent with what is known about structures in the local Universe (Bolejko 2005) or the observation of baryon oscillations in the matter power spectrum. Here we concern ourselves only with the CMB.

The picture of the local Universe that we adopt is a spherically symmetric density distribution, with the LG falling towards the core of the overdensity at the centre. The line between our location and the centre defines a preferred direction  $\hat{\mathbf{z}}$ , which in the present case corresponds to the direction of the dipole after subtracting our motion with respect to the LG and the LG’s infall towards the nearby Virgo cluster (assuming the primordial component of the dipole to be negligible). The directions on the sky that are important for our analysis are given in Table 1. This setup exhibits rotational symmetry w.r.t. the axis  $\hat{\mathbf{z}}$  (neglecting transverse components of our motion). Consequently, only zonal harmonics ( $m = 0$  in the  $\hat{\mathbf{z}}$ -frame) are generated.

The density field has two effects on the CMB seen by an off-centre observer. First, photons coming from different directions travel different routes through the local overdensity, and this creates anisotropy (even with a perfectly homogeneous distribution of photons). In a stationary setup (i.e. for virialised structures) this effect vanishes and there is no imprint on the CMB. Second, the environment will affect the evolution of the intrinsic anisotropies (as the homogeneous background space does, by changing the angular diameter distance). The correct calculation that would account for both of these effects would be to study the evolution of the CMB anisotropies as they travel across the density field using perturbation theory on the LTB background. We will present the calculation of the amplitude of the anisotropies induced by a local structure described with the LTB model elsewhere. As in earlier treatments, we neglect the second effect and simply add the anisotropy generated by the LTB model on top of the intrinsic contribution. It is possible that this treatment misses some effects

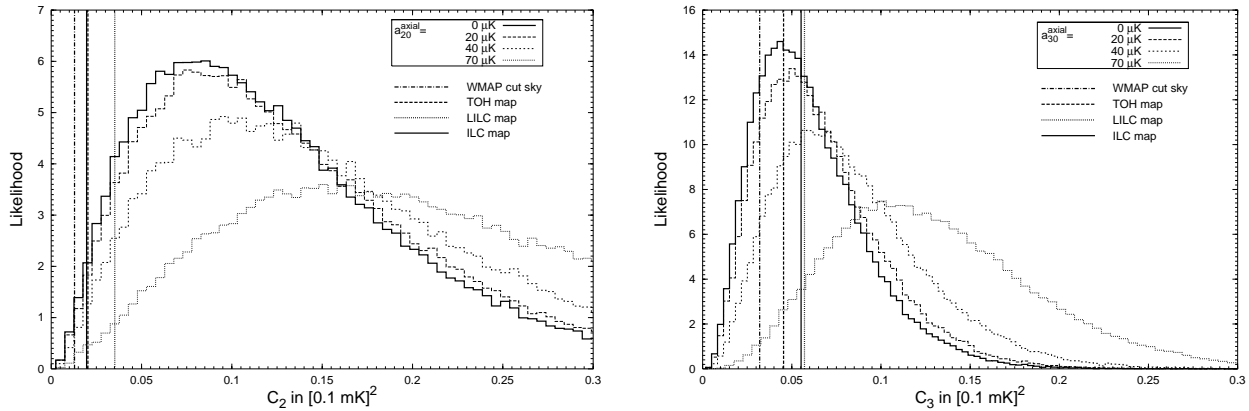


**Figure 1.** Likelihood of quadrupole and octopole power with increasing axial contamination. Vertical lines indicate measured values as given in Table 2. From the WMAP cut-sky analysis, adding *any* multipole power to the quadrupole is already excluded at  $> 99\%$ C.L., whereas it is possible to add up to  $80 \mu\text{K}$  to the octopole until reaching the same exclusion level.

of processing the anisotropies already present. In particular, simply linearly adding a new source of anisotropy will in general add multipole power, not reduce it, while a proper analysis of the processing of the intrinsic anisotropies could lead to a multiplicative modification of the amplitudes of the low multipoles, discussed in Gordon et al. (2005).

Any other effect with axial symmetry would also induce anisotropy only for the  $m = 0$  components. It has been suggested that spherically symmetric inhomogeneities of the order of horizon size or larger would contribute to the low CMB multipoles (Grishuck & Zel’dovich 1978; Raine & Thomas 1981; Paczyński & Piran 1990; Langlois & Piran 1996); it was claimed in Moffat (2005) that this could explain the observed preferred axis. Leaving aside the issue that assuming spherical symmetry for the entire Universe seems questionable, the observational signature on the low multipoles is identical to that from the LTB model used to describe local structures, possibly apart from the amplitude.

We study how the CMB is affected by the anisotropy induced by the additional axisymmetric contribution by means of Monte Carlo (MC) maps. We keep the amplitudes as free parameters to cover both local and horizon-sized structures at the same time, and look at how the observational signature compares with what is actually seen on the sky.

The angular power spectrum is given by  $C_\ell = \sum_m |a_{\ell m}|^2 / (2\ell + 1)$ , where  $a_{\ell m}$  are the coefficients in the harmonic decomposition of the temperature map. As predicted by the simplest inflationary models, we assume that the  $a_{\ell m}$  are statistically independent (isotropy), gaussian and have zero mean. The  $a_{\ell m}$  are then fully characterised by angular power. We use the values  $C_2 = 1278.9 \mu\text{K}^2$ ,  $C_3 = 590.9 \mu\text{K}^2$  from the best-fitting temperature spectrum of the  $\Lambda$  cold dark matter (ACDM) model with a power-law primordial perturbation spectrum to the combined WMAP, Cosmic Background Imager (CBI) and Arcminute Cosmology Bolometer Array Receiver (ACBAR) dataset. § For the statistical analysis we generate  $10^5$  MC realizations of the quadrupole and the octopole. As the contribution of the structure described by the LTB model, we

add to the quadrupole and the octopole a component, denoted by  $a_{\ell 0}^{\text{axial}}$ , which is a pure  $m = 0$  mode with respect to a given physical direction  $\hat{\mathbf{z}}$ .

First we address the amplitude of the quadrupole and the octopole. The values of  $C_2$  and  $C_3$  determined from the WMAP cut-sky (Hinshaw et al. 2003), the TOH map (Tegmark et al. 2003), the Lagrange ILC map (Eriksen et al. 2004b) and the Internal Linear Combination (ILC) map (Bennett et al. 2003b) are listed in Table 2. The extracted quadrupoles have been Doppler-corrected as described in Schwarz et al. (2004), except for the cut-sky value. The values of  $C_2$  and  $C_3$  from the full-sky maps are significantly larger than the cut-sky values.

Figure 1 shows how the  $C_2$  and  $C_3$  histograms compare with the data as  $a_{\ell 0}^{\text{axial}}$  is increased. For  $a_{\ell 0}^{\text{axial}} = 40 \mu\text{K}$ , the number of MC hits that are consistent with the WMAP cut-sky data is smaller by a factor of  $\sim 2$  for both  $C_2$  and  $C_3$  compared with the pure CMB sky. For  $a_{\ell 0}^{\text{axial}} = 70 \mu\text{K}$ , the number of consistent MC hits for  $C_2(C_3)$  is reduced by a factor of  $\sim 5(15)$  compared with the pure CMB sky. Note that adding *any* power to the theoretically expected quadrupole is excluded at the  $> 99\%$ C.L. level from the cut-sky analysis, but for the octopole the same exclusion level is not reached until  $a_{30}^{\text{axial}} = 80 \mu\text{K}$ .

Next we ask what kind of directional patterns the contribution  $a_{\ell 0}^{\text{axial}}$  induces on the sky. In the multipole vector representation (Copi et al. 2004) any real multipole  $T_\ell$  on a sphere (with radial unit vector  $\hat{\mathbf{e}}$ ) can be expressed with  $\ell$  unit vectors  $\hat{\mathbf{v}}^{(\ell, i)}$  and one scalar  $A^{(\ell)}$  as

$$T_\ell = \sum_{m=-\ell}^{\ell} a_{\ell m} Y_{\ell m}(\theta, \phi) \simeq A^{(\ell)} \prod_{i=1}^{\ell} \hat{\mathbf{v}}^{(\ell, i)} \cdot \hat{\mathbf{e}}. \quad (2)$$

The signs of the multipole vectors can be absorbed into the scalar quantity  $A^{(\ell)}$ , and are thus unphysical. Note that in (2) the r.h.s. contains contributions with angular momentum  $\ell - 2, \ell - 4, \dots$ . The uniqueness of the multipole vectors is ensured by removing these terms by taking the appropriate traceless symmetric combination (Copi et al. 2004). Note that the multipole vectors are independent of the angular power. As in Schwarz et al. (2004), we introduce the  $\ell(\ell - 1)/2$  oriented areas  $\mathbf{w}^{(\ell, i, j)} \equiv \hat{\mathbf{v}}^{(\ell, i)} \times \hat{\mathbf{v}}^{(\ell, j)}$ . Alignment

§ WMAP data products at <http://lambda.gsfc.nasa.gov/>

of the normals  $\mathbf{n}^{(\ell;i,j)} \equiv \pm \hat{\mathbf{w}}^{(\ell;i,j)}$  with a given direction  $\hat{\mathbf{x}}$  is tested with

$$S_{\mathbf{n}\mathbf{x}} \equiv \frac{1}{4} \sum_{\ell=2,3} \sum_{i<j} \left| \mathbf{n}^{(\ell;i,j)} \cdot \hat{\mathbf{x}} \right|. \quad (3)$$

This statistic is a sum over all dot products for a given  $\hat{\mathbf{x}}$ , so it does not imply any ordering between the terms and is a unique and compact quantity. For computing the multipole vectors we use the method introduced by Copi et al. (2004).<sup>¶</sup>

We look for alignment with three different directions  $\hat{\mathbf{x}}$ : the north ecliptic pole (NEP), the EQX and the north galactic pole (NGP). The first two are preferred directions in the Solar system and the last defines the plane of the dominant foreground. The observed  $S$ -values from the different CMB maps are given in Table 2. The results of the correlation analysis are shown in Fig. 2. By chance the CMB dipole and EQX lie very close to each other, so an alignment test with the dipole would give results very similar to the one with the EQX.

In the first row of Fig. 2 the preferred axis  $\hat{\mathbf{z}}$  is chosen to be the measured WMAP dipole (Bennett et al. 2003a). For all three tests the anomaly gets clearly worse, i.e. the axial mechanism drives the histograms away from the data. Next, instead of using the motion of the LG with respect to the CMB rest frame (Kogut et al. 1993) as the test direction, we take the velocity of the LG when corrected for Virgocentric motion (Plionis & Kolokotronis 1998), since this differs more from the WMAP dipole. The results are shown in the second row of Fig. 2. The situation for the alignment with the EQX is again worse, but there is not much effect on the ecliptic alignment. For the alignment with the galactic plane, the axial contribution makes an apparent Galactic correlation more probable, i.e. there is a certain probability of overestimating the galactic foreground. For both test directions (rows one and two), the alignment with the EQX gets worse. For example, in the direction of the Virgo-corrected LG motion an exclusion of  $\sim 99.9\%$  C.L. for  $a_{\ell 0}^{\text{axial}} = 50 \mu\text{K}$  can be given for all three maps. Note that adding *any* multipole power in this test can already be excluded at the  $\geq 99.4\%$  C.L.

As a complementary test we show the alignment likelihood with regard to an orthogonal test direction, the NEP, in row three of Fig. 2. An ecliptic extra contribution in the CMB would indeed induce an alignment of normal vectors similar to the observed one. In particular, for  $a_{\ell 0}^{\text{axial}} = 50 \mu\text{K}$ , the probability of finding an alignment with the NEP itself becomes roughly 5%, and the probability for the EQX alignment rises to 1%.

To summarise, the results of recent X-ray cluster studies indicate the existence of large-scale fluctuations  $\delta \simeq \mathcal{O}(1)$  at distances of  $\sim 100 h^{-1} \text{Mpc}$ . The local RS effect on the primordial photons from these structures is estimated to be of order  $\sim 10^{-5}$  at large angular scales. This raises the question of whether the local RS effect can account for the observed anomalies in the low multipoles of the CMB.

In this letter we have assumed spherical symmetry of the local superstructure, with an object like the Shapley Supercluster at the centre. Under this assumption we should

**Table 2.** Tests, defined in (3) and explained in the text, applied to the TOH, Lagrange ILC and ILC maps. All quadrupoles except the cut-sky value have been Doppler-corrected.

	Cut sky	TOH map	LILC map	ILC map
$C_2$	129 $\mu\text{K}^2$	203 $\mu\text{K}^2$	352 $\mu\text{K}^2$	196 $\mu\text{K}^2$
$C_3$	320 $\mu\text{K}^2$	454 $\mu\text{K}^2$	571 $\mu\text{K}^2$	552 $\mu\text{K}^2$
$S_{\mathbf{n}\text{NEP}}$	-	0.194	0.193	0.210
$S_{\mathbf{n}\text{EQX}}$	-	0.886	0.866	0.870
$S_{\mathbf{n}\text{NGP}}$	-	0.803	0.803	0.810

observe an axisymmetric effect on the microwave sky. The preferred axis has been taken to point in the direction of the local velocity flow (not shown in Fig. 2), the CMB dipole and the Virgo-corrected LG flow vector. We have added this axisymmetric contribution to a statistically isotropic gaussian random map and compared it by means of the  $S$ -statistic with WMAP measurements. The result is that this mechanism can be excluded at  $> 99\%$  C.L. Our analysis also applies to any other effect which gives an axisymmetric addition to the statistically isotropic and gaussian random sky. However, we find that a Solar system effect would be consistent with the data, in agreement with Copi et al. (2005).

The present work also indicates that the local Rees-Sciama effect might be important for the interpretation of WMAP data and future PLANCK data on the largest angular scales. Our work suggests that a more detailed study of the Rees-Sciama effect could lead to useful constraints on the local large-scale structure of the Universe.

Supplementary figures, illustrating the RS-induced CMB correlations, are available at <http://www.physik.uni-bielefeld.de/cosmology/rs.html>.

## ACKNOWLEDGMENTS

We thank J. Binney, C. Copi, G. Dalton, R. Davies, D. Huterer, S. Sarkar, G. Starkman and D. Wiltshire for discussions and comments. We acknowledge the use of the Legacy Archive for Microwave Background Data Analysis (LAMBDA) provided by the NASA Office of Space Science. The work of SR was partly done at the Rudolf Peierls Centre for Theoretical Physics at the University of Oxford, supported by PPARC grant PPA/G/O/2002/00479. The work of AR was supported by the DFG grant GRK 881.

## REFERENCES

- Alnes H., Amarzguioui M., Gron O., 2005, preprint (astro-ph/0512006)
- Bennett C.L. et al., 2003a, ApJS 148, 1
- Bennett C.L. et al., 2003b, ApJS 148, 97
- Bolejko, K., 2005, preprint (astro-ph/0512103)
- Célérier M.-N., 1999, A&A 353, 63
- Cooray A., Seto N., 2005, JCAP 0512, 004
- Copi C.J., Huterer D., Starkman G.D., 2004, PRD 70, 043515
- Copi C.J., Huterer D., Schwarz D.J., Starkman G.D., 2005, MNRAS in press, preprint (astro-ph/0508047)

<sup>¶</sup> Code at <http://www.phys.cwru.edu/projects/mpvectors/>

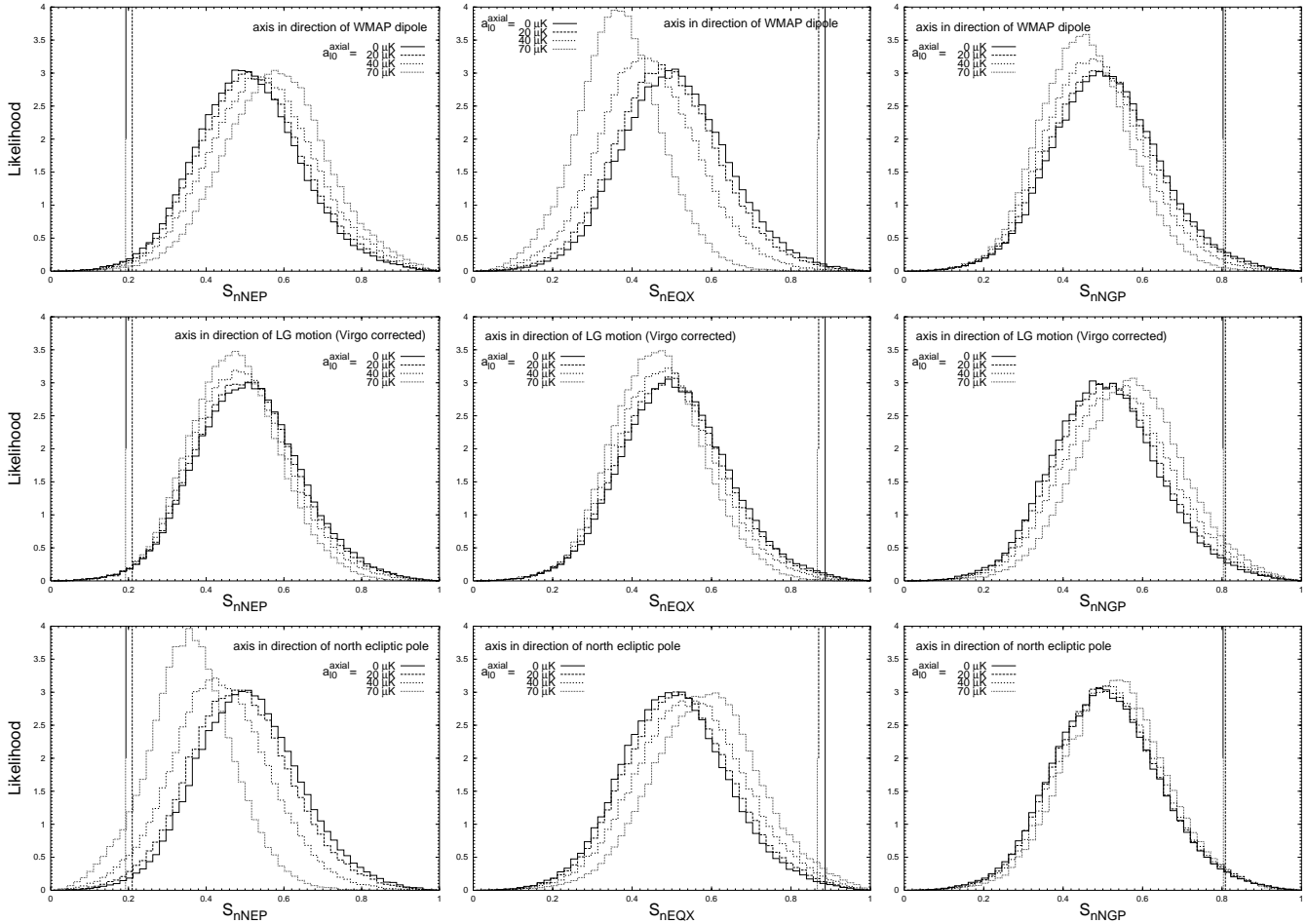


**Figure 2.** Alignment statistic (3) for quadrupole and octopole normals. For the three columns we pick the test direction  $\hat{\mathbf{x}}$  to be NEP, EQX and NGP respectively. In rows we consider three different choices of the preferred axis  $\hat{\mathbf{z}}$ , namely the WMAP dipole, the direction of motion of the LG, corrected for its Virgo infall, and the direction of the NEP. Shown are the likelihoods of the  $S$ -statistic for statistically isotropic gaussian skies (thick solid lines) as well as different magnitudes of axial contamination of the CMB (solid line), LILC (dotted line) and ILC (dashed line) maps (see Table 2). Vertical lines represent the measured  $S$ -values from the TOH (solid line), LILC (dotted line) and ILC (dashed line) maps. Introducing a preferred axis induces correlations. For the directions of local motion (first and second rows) these correlations make the discrepancy between the measured  $S$ -values and model even bigger. At the same time, a Solar system effect is more consistent with data.

de Oliveira-Costa A., Tegmark M., Zaldarriaga M., Hamilton A., 2004, PRD 69, 063516  
 Dressler A., 1988, ApJ 329, 519  
 Einasto M., Tago E., Jaaniste J., Einasto J., Andernach H., 1997, A&A Suppl. Ser. 123, 119  
 Eriksen H.K., Hansen F.K., Banday A.J., Górski K.M., Lilje P.B., 2004a, ApJ 605, 14, erratum ApJ 609, 1198  
 Eriksen H.K., Banday A.J., Górski K.M., Lilje P.B., 2004b, ApJ 612, 633  
 Freeman P.E., Genovese C.R., Miller C.J., Nichol R.C., Wasserman L., 2006, ApJ 638, 1  
 Fullana M.J., Sáez D., Arnau J.V., 1994, ApJS 94, 1  
 Gordon C., Hu W., Huterer D., Crawford T., 2005, PRD 72, 103002  
 Grishuck, L.P., Zel'dovich, I.B., 1978, Astron. Zh. 55, 209 [Sov. Astron. 22, 125]  
 Hinshaw G., Banday A.J., Bennett C.L., Gorski K.M., Kogut A., Lineaweaver C.H., Smoot G.F., Wright E.L., 1996, ApJ 464, L25  
 Hinshaw G. et al., 2003, ApJS 148, 63

Hudson M.J., Smith R.J., Lucey J.R., Branchini E., 2004, MNRAS 352, 61  
 Humphreys N.P., Maartens R., Matrauers D.R., 1997, ApJ 477, 47  
 Kocevski D.D., Mullis C.R., Ebeling H., 2004, ApJ 608, 721  
 Kocevski D.D., Ebeling H., 2005, preprint (astro-ph/0510106)  
 Kogut A. et al., 1993, ApJ, 419, 1  
 Krasinski A., 1997, Inhomogeneous Cosmological Models, Cambridge University Press, Cambridge  
 Langlois D., Piran T., 1996, PRD 53, 2908  
 Lucey J., Radburn-Smith D., Hudson M., 2004, preprint (astro-ph/0412329)  
 Lynden-Bell D., Faber S.M., Burstein D., Davies R.L., Dressler A., Terlevich R.J., Wegner G., 1988, ApJ 326, 19  
 Mansouri R., 2005, preprint (astro-ph/0512605)  
 Martínez-González E., Sanz J.L., 1990, MNRAS 247, 473  
 Moffat J.W., 2005, JCAP 0510, 012

- Paczynski B., Piran T., 1990, ApJ 364, 341  
Panek, M., 1992, ApJ 388, 225  
Plionis M., Kolokotronis V., 1998, ApJ 500, 1  
Proust D. et al., 2006, A&A 447, 133  
Raine D.J., Thomas E.G., 1981, MNRAS 195, 649  
Rees M.J., Sciama D.W., 1968, Nature 217, 511  
Sáez D., Arnau J.V., Fullana M.J., 1993, MNRAS 263, 681  
Schwarz D.J., Starkman G.D., Huterer D., Copi C.J., 2004,  
PRL 93, 221301  
Seljak, U., 1996 ApJ 460, 549  
Tegmark M., de Oliveira-Costa A., Hamilton A.J.S., 2003,  
PRD 68, 123523  
Tomita K., 2001, Prog. Theor. Phys. 106, 929  
Tomita K., 2005a, PRD 72, 043526  
Tomita K., 2005b, PRD 72, 103506  
Vale C., 2005, preprint (astro-ph/0509039)